LU TP 96-30
December 23, 1996

The Electrostatic Persistence Length Calculated from Monte Carlo, Variational and Perturbation Methods

Magnus Ullner[1] and Bo Jönsson[2]
Physical Chemistry 2, Chemical Center, University of Lund
Box 124, S-221 00 Lund, Sweden

Carsten Peterson[3], Ola Sommelius[4] and Bo Söderberg[5]
Complex Systems Group, Department of Theoretical Physics
University of Lund, Sölvegatan 14A, S-223 62 Lund, Sweden

Submitted to *Journal of Chemical Physics*

Abstract:

Monte Carlo simulations and variational calculations using a Gaussian ansatz are applied to a model consisting of a flexible linear polyelectrolyte chain as well as to an intrinsically stiff chain with up to 1000 charged monomers. Addition of salt is treated implicitly through a screened Coulomb potential for the electrostatic interactions.

For the flexible model the electrostatic persistence length shows roughly three regimes in its dependence on the Debye-Hückel screening length, κ^{-1}. As long as the salt content is low and κ^{-1} is longer than the end-to-end distance, the electrostatic persistence length varies only slowly with κ^{-1}. Decreasing the screening length, a controversial region is entered. We find that the electrostatic persistence length scales as $\sqrt{\xi_p}/\kappa$, in agreement with experiment on flexible polyelectrolytes, where ξ_p is a strength parameter measuring the electrostatic interactions within the polyelectrolyte. For screening lengths much shorter than the bond

[1]fk2mul@dix.fkem2.lth.se
[2]fk2boj@grosz.fkem2.lth.se
[3]carsten@thep.lu.se
[4]ola@thep.lu.se
[5]bs@thep.lu.se

length, the κ^{-1} dependence becomes quadratic in the variational calculation. The simulations suffer from numerical problems in this regime, but seem to give a relationship half-way between linear and quadratic.

A low temperature expansion only reproduces the first regime and a high temperature expansion, which treats the electrostatic interactions as a perturbation to a Gaussian chain, gives a quadratic dependence on the Debye length.

For a sufficiently stiff chain, the persistence length varies quadratically with κ^{-1} in agreement with earlier theories.

I. INTRODUCTION

During the last decade or so a large number of simulations of charged polymers have appeared in the literature. Many of these have been devoted to the study of conformational properties in bulk solution,[1–6] while a few have focused on the dramatic effects polyelectrolytes can produce in charged colloidal dispersions.[7,8] In the former case the polymer chain is quite often characterized by a few geometric parameters like the end-to-end separation or the radius of gyration. The behaviour of a polyelectrolyte has also been analyzed in terms of its persistence length. The subject of persistence length may sometimes appear confusing due to the number of definitions and different ways to calculate the quantity. The general concept of persistence length is however the same — it is a measure of stiffness, a characteristic length over which a polymer chain remembers its direction. Of course, even a neutral polymer will have a non-zero persistence length and it has become common practice to divide the total persistence length into an electrostatic, $l_{p,e}$, and a non-electrostatic or "bare" part, $l_{p,0}$,

$$l_{p,t} = l_{p,0} + l_{p,e}. \tag{1}$$

Odijk[9] and, independently, Skolnick and Fixman[10] (OSF) derived equivalent models to calculate the influence of electrostatic interactions on the persistence length and in particular the effect of screening from added salt. For some time there has been a controversy in the literature over conflicting results for the ionic strength dependence[11–14] and it is the purpose of this communication to resolve the conflict.

Experimentally the OSF result, which suggests a quadratic dependence on the Debye length, κ^{-1}, for the electrostatic persistence length, has been confirmed for intrinsically very stiff polyelectrolytes, like DNA[15] and poly(xylylene tetrahydrothiophenium chloride)[16], but although it has been claimed that the theory is also valid for long, flexible chains,[17,18] the experimental findings generally points towards a linear relationship, i.e. $l_{p,e} \sim \kappa^{-1}$, for flexible polyelectrolytes.[19–22] An objection to the OSF theory is the neglect of entropy. Taking this into account, variational calculations also give the linear relationship.[23,11,12] Simulations usually show deviations from the OSF theory, and the exponent p in $l_{p,e} \sim \kappa^{-p}$ may vary from 1.5[24] down to 0.3-0.9[13]. However, $p \approx 1$, in agreement with experiment, have also been reported.[3,6]

It is our conclusion that an almost linear relationship does exist for a flexible polyelectrolyte when the screening length is shorter than the dimensions of the chain, but longer than the monomer-monomer separation. For an intrinsically stiff chain, however, we find a quadratic dependence in agreement with the OSF theory.

II. THE PERSISTENCE LENGTH

Prior to discussing the models and our different approaches we review different definitions of the persistence length and briefly discuss the OSF theory. Given a linear chain with N monomers, the microscopic approach to the persistence length is simply to sum the average scalar products of bond vectors with respect to a certain bond, i.e. to calculate the average sum of directional cosines,

$$l_{p,i} = \frac{1}{a} \sum_{k=0}^{N-1-i} \langle \mathbf{r}_i \cdot \mathbf{r}_{i+k} \rangle = a \sum_{k=0}^{N-1-i} \langle \cos\theta_{i+k} \rangle. \tag{2}$$

where $\mathbf{r}_i = \mathbf{x}_{i+1} - \mathbf{x}_i$ is the bond vector between monomer i and $i+1$, whereas $\mathbf{x}_i$ represents the coordinate of monomer i and a is an average bond length. In the following a will represent the root-mean-square monomer-monomer separation,

$$a^2 = \frac{1}{N-1} \sum_{j=1}^{N-1} \langle \mathbf{r}_j^2 \rangle, \tag{3}$$

which, of course, is the same as the bond length for a chain with rigid bonds. Usually, i denotes the central bond and the cosines are calculated from the average of the scalar products in both directions and not just for subsequent bonds as written in Eq. (2). One may also calculated $l_{p,N/2}$ as an average over both directions. The average over all the local and uni-directional persistence lengths, $l_{p,i}$, is related to the mean-square end-to-end separation,

$$R_{ee}^2 \equiv \langle (\mathbf{x}_N - \mathbf{x}_1)^2 \rangle = \langle \sum_{i=1}^{N-1} \mathbf{r}_i \cdot \sum_{j=1}^{N-1} \mathbf{r}_j \rangle = \sum_{i=1}^{N-1} \langle \mathbf{r}_i^2 \rangle + 2 \sum_{i=1}^{N-2} \sum_{j=i+1}^{N-1} \langle \mathbf{r}_i \cdot \mathbf{r}_j \rangle, \tag{4}$$

i.e.

$$l_{p,R} \equiv \frac{1}{N-1} \sum_{i=1}^{N-1} l_{p,i} = \frac{R_{ee}^2}{2(N-1)a} + \frac{a}{2}. \tag{5}$$

In the case of an infinite chain, all bonds are equivalent and so are the persistence lengths of Eqs. (2) and (5). We may in fact treat the polymer as infinite and disregard the index i in Eq. (2), if the chain is long enough to make end-effects unimportant, i.e., for most bonds $\langle \cos\theta_{i+k} \rangle$ will become zero before k reaches the end and most of the chain will be described by the same orientational correlation function, C_k. This function is normally expected to to decay exponentially with a characteristic length scale, $l_{p,x}$,

$$C_k \equiv \langle \cos\theta_k \rangle = \mathrm{e}^{-ka/l_{p,x}}. \tag{6}$$

Planning ahead, we might be tempted to fit the correlation function to an exponential function, e.g. by linear regression of $\ln C_k$ *vs.* k, and simply calculate $l_{p,x}$ from the slope in this case. This is not such a good idea, however, because we are disregarding one of the fitting parameters. It is a little optimistic to think that the fitting would reproduce the exact value, $C_0 = 1$, as the prefactor of the exponential (or the intercept $\ln C_0 = 0$ in the linear regression). In order to take both parameters into account, it is better to integrate

$$l_{p,\infty} = a \int_0^\infty C_0 \mathrm{e}^{-ka/l_{p,x}}\, dk = C_0 l_{p,x}. \tag{7}$$

We see that when $C_0 = 1$ we get $l_{p,x}$ back and at the same time we have a natural way to incorporate a fitted $C_0 \neq 1$. The integral is essentially the sum in Eq. (2) and here we have the connection between the microscopic and exponential definitions. There is a difference, however. The sum in Eq. (2) is truncated at the end of the chain regardless if C_k has decayed to zero or not, while the integral in Eq. (7) extrapolates the result to that of an infinite chain. The significance of this will become evident when we look at the results.

The correlation function C_k is discrete since we are considering a polymer with discrete bonds. We will get a continuous function, however, if we make the bonds or segment lengths infinitesimally small, $a \to ds$, and the number of segments infinitely large, while keeping the contour length, $L = (N-1)a = \sum_{i=1}^{N-1} a = \int_0^L ds$, fixed. This is the worm-like chain model.[25,26] In the chain with discrete bonds there is automatically an intrinsic stiffness, even in the absence of interactions. This results, in the well-known mean-square end-to-end distance for a freely jointed chain or random walk with a fixed step length a,

$$R_{ee}^2 = \sum_{i=1}^{N-1} a^2 C_0 + 2 \sum_{k=1}^{N-1} (N-1-k) a^2 C_k = (N-1)a^2, \tag{8}$$

since there are $N-1-k$ scalar products of the type $\langle \mathbf{r}_i \cdot \mathbf{r}_{i+k} \rangle$ [cf. Eq. (4)] and without interactions one has

$$C_k = \begin{cases} 1 & \text{for } k = 0 \\ 0 & \text{otherwise} \end{cases} . \tag{9}$$

For the worm-like chain we need to specify $C(s) \equiv \langle \cos\theta(s) \rangle$, where $s = \int_0^s ds$ is a distance along the contour of the chain, in order to calculate [cf. Eq. (8)]

$$R_{ee}^2 = 2 \int_0^L (L-s)\, C(s)\; ds. \tag{10}$$

Returning to the assumption of an exponential decay, i.e. $C(s) = \exp\left(-s/l_{p,w}\right)$, we get

$$R_{ee}^2 = 2Ll_{p,w} - 2l_{p,w}^2 \left(1 - \mathrm{e}^{-L/l_{p,w}}\right). \tag{11}$$

If R_{ee} is known, $l_{p,w}$ can be obtained from 11. This method is often used to extract an apparent persistence length from experimental data,[27,3,21] although what is usually measured is the radius of gyration, R_G, defined as

$$R_G^2 \equiv \frac{1}{N} \sum_{i=1}^{N} \langle (\mathbf{x}_i - \mathbf{x}_{cm})^2 \rangle = \frac{1}{N^2} \sum_{i=1}^{N} \sum_{j=i+1}^{N} \langle x_{ij}^2 \rangle, \tag{12}$$

where $\mathbf{x}_{cm}$ is the centre of mass coordinate and x_{ij} is the distance between atoms i and j. The worm-like chain expression used is

$$R_G^2 = \frac{2}{L^2}\int_0^L ds'\,(L-s')\int_0^L ds\,(s'-s)\,\mathrm{e}^{-L/l_{p,w}} = \frac{Ll_{p,w}}{3} - l_{p,w}^2 + 2\frac{l_{p,w}^3}{L} - 2\frac{l_{p,w}^4}{L^2}\left(1-\mathrm{e}^{-L/l_{p,w}}\right) \tag{13}$$

or its long chain limit ($L \gg l_{p,w}$)

$$R_G^2 \approx \frac{Ll_{p,w}}{3}. \tag{14}$$

For a worm-like chain with an exponentially decaying correlation function, Eqs. (11) and (13) are equivalent. In other cases the obtained persistence lengths would hardly be identical, but the trends are expected to be the same. For convenience we will be using Eq. (11).

The persistence lengths discussed above are all total persistence lengths, where the "bare" part, the persistence length in the absence of electrostatic interactions, depends on the chain (model) itself. For example, for the freely jointed chain $l_{p,0}$ is equal to the bond length [cf. Eqs. (5) and (8)] and, experimentally, a value extrapolated to infinite amounts of salt is often used. In order to calculate the electrostatic part, the OSF theory considers the electrostatic contribution to the bending energy, which is quadratic in the curvature or bending angle, for a very stiff worm-like chain ($l_{p,0} \gg \kappa^{-1}$), whose electrostatic interactions are described by the Debye-Hückel approximation, i.e. a screened Coulomb potential

$$u_{sc}(r) = k_B T l_B \frac{\mathrm{e}^{-\kappa r}}{r}, \tag{15}$$

where k_B is Boltzmann's constant, T is the absolute temperature and $l_B = e^2/(4\pi\epsilon_r\epsilon_0 k_B T)$ is the Bjerrum length, with e the elementary charge, ϵ_r the dielectric constant of the solution and ϵ_0 the permittivity of vacuum. The Debye screening length, κ^{-1}, is given by $\kappa^2 = 8\pi l_B N_A I 1000$, where N_A is Avogadro's number and I is the ionic strength in units of molar concentration (SI units are implied for the other quantities). The Debye-Hückel approximation is expected to be reasonable for a 1:-1 salt (and a weakly charged polyelectrolyte), in which case the ionic strength is just the molar salt concentration, i.e. $I = C_s$. The predicted electrostatic persistence length is

$$l_{OSF} = \frac{l_B Z^2}{12}\left[3y^{-2} - 8y^{-3} + \mathrm{e}^{-y}(y^{-1} + 5y^{-2} + 8y^{-3})\right], \tag{16}$$

with $y \equiv \kappa L$ and Z the amount of elementary charges on the chain. For large y this reduces to

$$l'_{OSF} = \frac{l_B}{4\kappa^2 A^2}, \tag{17}$$

where $A = L/Z$ is the length per unit charge. If we translate this to a model with a certain bond length a and a charge per monomer $\alpha = Z/N$ we get

$$l'_{OSF} = \frac{\alpha^2 l_B}{4\kappa^2 a^2}. \tag{18}$$

Besides the bond interactions, the models used in the simulations of the flexible polyelectrolyte chains only contain electrostatic interactions, which allows us to obtain a truly *electrostatic* persistence length. In the simulations of the stiff polyelectrolyte chains we also include a bond angle term. In a real polyelectrolyte other interactions, like excluded volume and attractive interactions, may be significant. Still, what we see here is in very good agreement with experiment.

III. MODELS

The polyelectrolyte is regarded as an infinitely diluted polyacid in a salt solution. The monomers form a linear chain where each monomer represents a charged site that carry one unit of negative charge. Three different models have been considered: Model 1 and 2 are freely jointed chains with harmonic and rigid bonds, respectively. In model 3 the rigid bonds have been augmented with an angular potential restricting the orientation of adjacent bonds. The harmonic bonds correspond to an approximately Gaussian distribution of bond lengths and can be viewed as an averaging over the conformational freedom of the covalent structure that implicitly joins the charged sites.

The solvent is treated as a dielectric continuum with a dielectric constant $\epsilon_r = 78.3$, corresponding to water at room temperature, and the salt ions are implicitly represented by the screening parameter κ. Thus, charged monomers interact via a screened Coulomb potential, E_C, which for the flexible bond model (model 1) is augmented with a Gaussian term, E_G, leading to a total interaction energy

$$E = E_G + E_C = \frac{k}{2} \sum_{i \neq N} r_{i,i+1}^2 + \frac{\alpha^2 e^2}{4\pi\epsilon_r\epsilon_0} \sum_i \sum_{j>i} \frac{\mathrm{e}^{-\kappa r_{i,j}}}{r_{i,j}}, \tag{19}$$

where N is the number of monomers, $r_{i,j}$ is the distance between monomer i and j, e is the electronic charge, ϵ_0 is the permittivity of vacuum and α the (fractional) amount of charge on a monomer i. The force constant, k, is given implicitly through the input parameter $r_0 = (e^2/4\pi\epsilon_r\epsilon_0 k)^{1/3}$, which is the equilibrium distance for a fully charged dimer.

The angular potential in model 3 is simply,

$$E_A = -k_B T \frac{l_B l_A^2}{r_0^3} \sum_{i=1}^{N-1} \cos\theta_i, \tag{20}$$

where θ_i is the angle between bond i and $i+1$. The angular potential is characterized by the length l_A and increasing l_A means increased stiffness in the chain.

IV. METHODS

The key approach employed for studying the scaling properties of the persistence length is the Monte Carlo method. In this section, however, we also discuss what is expected from non-stochastic approaches; a variational method, high- and low-T expansions.

A. Monte Carlo simulation

The Monte Carlo (MC) simulations were performed with the traditional Metropolis algorithm[28] in a canonical ensemble. One polyelectrolyte chain at infinite dilution was simulated. The sampling of chain conformations was made highly efficient, compared to traditional Monte Carlo moves, by using a pivot algorithm, which allows chain lengths of more than 2000 monomers. The pivot algorithm was first described by Lal,[29] and its efficiency for self-avoiding walks have been thoroughly discussed by Madras and Sokal.[30] Despite its excellent properties, it was only recently that the pivot algorithm started to gain wider recognition as a tool to enhance simulations of polymers and polyelectrolytes.[31,24,32,33]

In a traditional single-move algorithm only one or a few monomers are translated or rotated at a time. The number of interactions that has to be calculated is of the order N and a large number of attempts per monomer is needed to generate independent chain conformations. Similarly, in the pivot algorithm each monomer i (except the first one) is translated in turn but together with the rest of the chain (monomers $i+1$ to N). Furthermore, the last part of the polymer is then rotated as a rigid body around one of the coordinate axes with monomer i as origin. To be specific, if the bonds are flexible (model 1) they are both translated and rotated, while in the case of rigid bonds (models 2 and 3) only the rotation is performed. The number of interactions calculated in one step is of the order N^2 but independent conformations are obtained after a only a few attempted moves, on the order of one per monomer or N in total. The net effect is a greatly reduced simulation time for a given degree of precision and a computational cost that grows approximately as N^3.

One expects the pivot algorithm to have its maximal efficiency for unscreened and extended chains, but we have recently shown its efficiency even for screened chains with less elongated structure.[34] The pivot algorithm provides an effective sampling of global properties like R_{ee}, but it turns out to be superior also for local properties like the monomer-monomer separation. A more detailed investigation than the present, is needed to really map out the applicable range for the pivot algorithm.

B. Variational approach

In the variational approach the true Boltzmann distribution $P \propto \exp(-E/k_BT)$ is approximated by a trial distribution $P_V \propto \exp(-E_V/k_BT)$, having a set of free parameters. It yields a variational free energy

$$\hat{F} = \langle E \rangle_V - k_BTS_V \geq F, \tag{21}$$

bounded from below by the true free energy F. $\langle E \rangle_V$ is the average of the true energy in the trial Boltzmann distribution P_V and S_V is the corresponding variational entropy. By minimizing $\hat{F}$ with respect to the parameters of E_V, thermodynamic quantities can be estimated. In the case of model 1 (flexible chain), we consider an arbitrary pure Gaussian variational distribution,[32] corresponding to

$$E_V/k_BT = \frac{1}{2}\sum_{ij} G_{ij}^{-1}\mathbf{r}_i \cdot \mathbf{r}_j, \tag{22}$$

where $\mathbf{r}_i$ denotes the ith bond vector. With the correlation matrix G optimized (numerically) so as to minimize $\hat{F}$, the variational estimate for the correlation matrix becomes

$$\langle \mathbf{r}_i \cdot \mathbf{r}_j \rangle_V = 3G_{ij}. \tag{23}$$

From this a variational estimate for the persistence length, e.g. as defined in Eq. (5), can be obtained.

C. High temperature expansion

For model 1 at high temperatures, the energy [Eq. (19)] will be dominated by the bond term, and the interaction E_C can be treated as a perturbation. A perturbative expansion for the thermal average of an arbitrary observable f yields

$$\langle f \rangle = \langle f \rangle^0 - \frac{1}{k_BT}\langle fE_C \rangle_C^0 + \frac{1}{2(k_BT)^2}\langle fE_CE_C \rangle_C^0 + \ldots, \tag{24}$$

where $\langle\,\rangle_C^0$ refers to connected expectation values in the unperturbed Boltzmann distribution.

In a continuum approximation, valid when the nearest-neighbour distance is small as compared to the range of the interaction, the first few terms in the perturbative expansion of the squared end-to-end distance R_{ee}^2 are given by[35] (assuming full charge, $\alpha = 1$)

$$\langle R_{ee}^2 \rangle = \frac{Nr_0^3}{l_B}\left[3 + \gamma f_1(\mu) + \gamma^2 f_2(\mu) + \ldots\right]. \tag{25}$$

where

$$f_1(\mu) = 4\sqrt{\frac{2}{\pi}} - 16\mu^{-1/2} + \mathcal{O}(\mu^{-1}) \ , \ \ f_2(\mu) = -\left(\frac{32}{\pi} - \frac{56}{9}\right) + \mathcal{O}(\mu^{-1/2}) \tag{26}$$

with the dimensionless parameters μ and γ given by

$$\mu = \frac{N\kappa^2 r_0^3}{l_B} \ , \ \ \gamma = \frac{N^{1/2} l_B^{5/2}}{\kappa^2 r_0^{9/2}}. \tag{27}$$

Note that μ is proportional to the squared unperturbed end-to-end distance in units of the screening length; in the parameter range we are studying, μ is large.

Keeping only the leading large-μ contribution to each term f_i yields a power series in γ, indicating that the expansion is valid for small γ. Unfortunately, for the parameter range we are studying γ is *not* small, and while the first order expansion is proportional to κ^{-2}, the next order term, proportional to κ^{-4}, is larger and has a negative value.

Similarly, for the average squared bond length we obtain in the continuum approximation the perturbative result

$$a^2 \equiv \langle r_{mm}^2 \rangle = \frac{r_0^3}{l_B}\left[3 + 4\frac{l_B^2}{\kappa r_0^3} + \ldots\right]. \tag{28}$$

The persistence length $l_{p,R}$ is then obtained by dividing R_{ee}^2 by $N r_{mm}$. In the results section, we have included the first order perturbative result for comparison, although a good agreement cannot be expected since the parameter γ is not small.

D. Low temperature expansion

A similar approach can be followed for low temperatures, where the Boltzmann distribution is dominated by the minimal energy configuration. For small fluctuations around the ground state, the energy can to lowest order be considered Gaussian, with the corrections treated as a perturbation. The resulting correlation matrix $\langle \mathbf{r}_i \cdot \mathbf{r}_j \rangle$[36] can be used to calculate the persistence length.

V. RESULTS AND DISCUSSION

A. Flexible polyelectrolyte

From the form of the Hamiltonian, being just a sum of screened Coulomb interactions [Eq. (15)], and the fact that the statistical mechanical weight of a conformation is given by $\exp(-E/k_BT)$, it is easy to see that the rigid bond model scales with the bond length a as the unit of length and that any scaled length, e.g. l_p/a, must be a function of the dimensionless numbers (scaled length scales) κa and the strength parameter

$$\xi_p = \frac{\alpha^2 l_B}{a}, \tag{29}$$

which measures the strength of the electrostatic interactions within the polyelectrolyte for a given N. As a visual proof, Fig. 1 shows that $l_{p,e}/a$ is constant for a given value of these parameters. Note that ξ_p is different from the so called Manning parameter,[37] $\xi = l_B/A = \alpha l_B/a$, which measures the interactions between the polyelectrolyte and mobile ions. In a previous paper we found for a titrating polyelectrolyte that the approximation of putting full charges a distance A apart is inferior to having fractional charges on the actual titrating sites.[38] Thus, we may conclude that ξ_p is the more pertinent parameter in this context.

The results in Fig. 2 show two distinct regimes in the salt dependence of the electrostatic persistence length. For low salt concentrations, i.e. when the Debye screening length is longer than the dimensions of the chain ($\kappa^{-1} \gg R_{ee}$), $l_{p,e}$ is almost constant. Note that the symbols on the y-axis represent the values in the unscreened case ($\kappa = 0$). When $\kappa^{-1} \ll R_{ee}$ the relationship between $l_{p,e}$ and κ^{-1} is close to linear. There is actually a third regime when κ^{-1} is less than the bond length, but we will save that till the discussion of the variational results.

Experimentally, Reed *et al.* have found a linear dependence on both κ^{-1} and α for $l_{p,e}$.[21] To us, this implies

$$l_{p,e} \sim \frac{\sqrt{\xi_p}}{\kappa} = \frac{\alpha}{\kappa}\sqrt{\frac{l_B}{a}} = \frac{\alpha}{\sqrt{8000\pi N_A I a}} \tag{30}$$

at high salt concentrations, which is confirmed in Figs. 3 and 4. Note that $l_{p,e}$ is predicted to be temperature independent. Ha and Thirumalai (HT) have derived a similar expression, $l_p \sim \sqrt{(l_{p,0} l_B/A^2)}/\kappa$ for $l_{OSF} \gg l_{p,0}$.[12] As long as $l_{p,0} = a$ the two expressions are the same, although l_p in their case appears to be the total persistence length. However, if we add a repulsive potential between next-nearest neighbours, which increases $l_{p,0}$ (but not too much, see below), Eq. (30) still holds, while the HT expression with the actual intrinsic persistence length does not. The slope for the highly screened regime ($\kappa^{-1} \ll R_{ee}$) in Fig. 4 is roughly -1.1.

Equation (30) has no N dependence. Naively one may expect excluded volume behaviour in the high salt regime as a result of short ranged electrostatic interactions between monomers, which can also be far apart in the sequence as the chain loops back on itself. For a self-avoiding chain we have $R_{ee}^2 \sim N^{1.2}a^2$,[39] which from Eq. (5) would suggest $l_{p,e} \sim N^{0.2}$ for long chains. The slopes of the linear parts of Fig. 3, roughly 2.6, 4.3 and 7.3 for $N = 80$, 320 and 1000, respectively, give an N-exponent of 0.4.

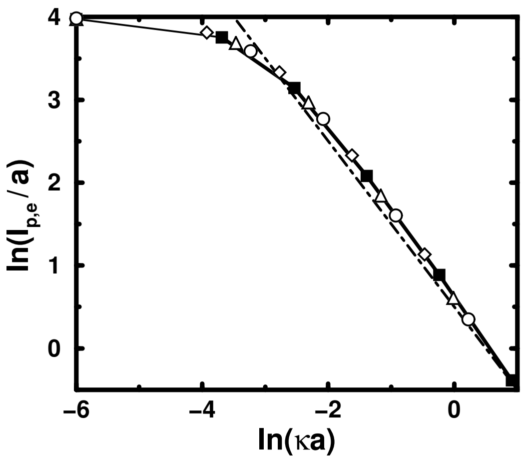

FIG. 1. The logarithm of the scaled electrostatic persistence length, where $l_{p,e} = l_{p,R} - a$ [cf. Eq. (5)], as a function of $\ln(\kappa a)$ for rigid bond chains with $N = 320$ and fixed ξ_p. Filled squares represent $a = 24$ Å and $\alpha = 1$ and the open symbols represent $\alpha/a = 0.3536/3$ Å (triangles), 0.5/6 Å (diamonds) and 0.707/12 Å (circles), with the values on the y-axis showing the results for the salt-free case. The dot-dashed line marks a slope of -1.

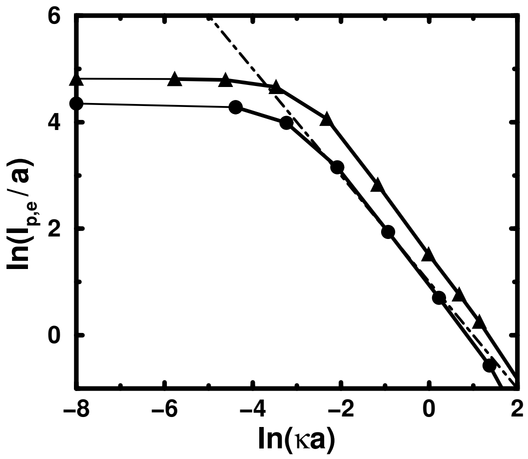

FIG. 2. The logarithm of the scaled electrostatic persistence length, where $l_{p,e} = l_{p,R} - a$ [cf. Eq. (5)], as a function of $\ln(\kappa a)$. The results are for rigid bond chains with $N = 320$ and $a = 3$ Å (triangles) and 12 Å (circles) and fully charged monomers. The values on the y-axis are for the salt-free case, and are connected to the rest of the points by thinner lines. The dot-dashed line denotes a slope of -1.

So far we have used the “macroscopic” persistence length, Eq. (5), but the same conclusions are reached with other definitions as can be seen in Table I and Fig. 5. The two persistence lengths obtained directly form the simulation, $l_{p,N/2}$ and $l_{p,R}$ [Eqs. (2) and (5)], are almost identical. $l_{p,R}$ is a global quantity and thus have better statistics than $l_{p,N/2}$, which has more local character. This becomes noticeable at high salt concentrations where the latter starts

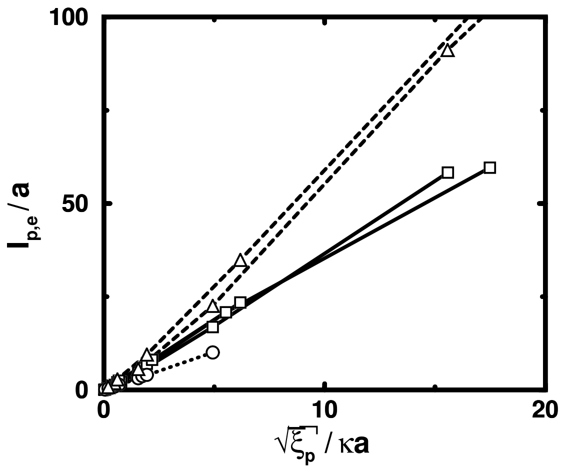

FIG. 3. The scaled electrostatic persistence length, where $l_{p,e} = l_{p,R} - a$, as a function of $\sqrt{\xi_p}/\kappa a$. The results are for rigid bond chains with $N = 80$ (circles) and 320 (squares) with bond lengths 3 Å, 6 Å, 12 Å and 24 Å as well as $N = 1000$ with $a = 3$ Å and 12 Å (triangles). In order to clearly show the linear regime, only points where $\kappa^{-1} \leq R_{ee}/10$ are displayed.

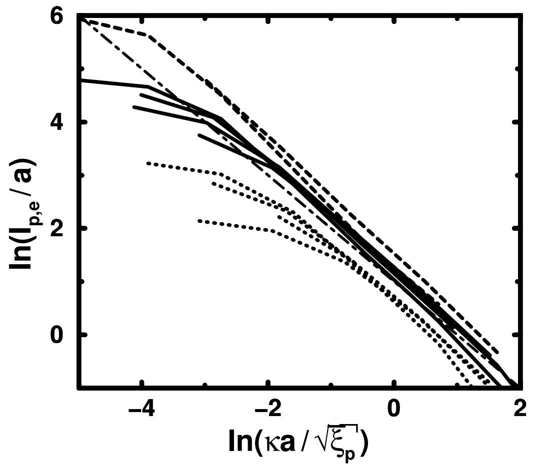

FIG. 4. The logarithm of the scaled electrostatic persistence length, where $l_{p,e} = l_{p,R} - a$, as a function of $\sqrt{\xi_p}/\kappa a$. The lines represent the same combinations of a and α as in 3. The dot-dashed line marks a slope of -1.

to suffer from insufficient averaging. The worm-like chain persistence length, Eq. (11), also give the same results for $\kappa^{-1} \ll R_{ee}$ and $\kappa^{-1} > a$. For screening lengths less than the bond length the true structure of the chain becomes important and the worm-like chain model breaks down and even gives negative persistence lengths. To save the worm-like chain, a term corresponding to the last term of Eq. (5) would have been needed in Eq. (11).

$l_{p,x}$ [Eq. (6)] and $l_{p,\infty}$ have been obtained by fitting an exponential to the orientational

TABLE I. End-to-end separation and electrostatic persistence lengths from different definitions, $l_{p,N/2} - a$ from Eq. (2), $l_{p,R} - a$ from Eq. (5), $l_{p,x} - a$ from Eq. (6), $l_{p,\infty} - a$ from Eq. (7), $l_{p,w} - a$ from Eq. (11) and l_{OSF} from Eq. (16), obtained for a 320-mer. The unit of length is 1 Å.

a	C_s/M	κ^{-1}	R_{ee}	$l_{p,N/2} - a$	$l_{p,R} - a$	$l_{p,x} - a$	$l_{p,\infty} - a$	$l_{p,w} - a$	l_{OSF}
	0	—	844	383	371	6969	5909	1182	10185
	0.00001	961	843	376	370	6494	5412	1169	9191
	0.0001	304	834	372	362	5246	4365	1071	5655
	0.001	96	781	334	317	2152	1713	699	1353
3	0.01	30	581	197	175	409	288	228	169
	0.1	9.6	316	58	51	117	56	52	18
	1	3.0	171	16	14	66	10	12	2
	10	0.96	101	5	4	52	-1	2	0.2
	100	0.30	68	0.9	0.9	62	-3	-0.6	0.02
	0	—	2680	1018	932	9158	5636	1433	10185
	0.00001	961	2586	943	867	7258	4231	1267	4605
	0.0001	304	2236	713	647	3300	1678	821	910
	0.001	96	1483	324	281	978	378	301	108
12	0.01	30	828	99	84	461	87	80	11
	0.1	9.6	481	27	24	256	14	18	1
	1	3.0	313	7	7	213	-11	0.8	0.1
	10	0.96	234	4	1	262	-12	-5	0.01
	100	0.30	217	1	0.2	420	-12	-6	0.001

correlation function. In order to avoid end-effects we have calculated C_k from the central bond and fitted the function only in the range k=0–120 (N=320). Figure 6 shows the correlation function together with the fitted exponential. It is clear that some information is lost at small values of k and that this is of greater importance at higher salt concentrations. In particular the initial part at $C_0 = 1$, which for the integrated persistence length $l_{p,\infty}$ corresponds to the intrinsic persistence length, $l_{p,0} = a$, is lost. Table I shows that if we did not subtract $l_{p,0}$ from $l_{p,\infty}$, this persistence length would be in good agreement with the microscopic definitions, not only at intermediate salt concentrations, but also at higher salt concentrations. Even more information is lost when calculating $l_{p,x}$. Note for example that the fitted exponentials have a prefactor (C_0) that is less than one and decreasing faster than C_1. In Fig. 5 we see that $l_{p,x}$ has a behaviour of its own. There is not a simple, consistent κ^{-1} dependence and an apparent exponent p in $l_{p,x} \sim \kappa^{-p}$ can have a range of values less than one, which is exactly the result of Micka and Kremer.[13] Their conclusions are thus a consequence of an unfortunate choice of persistence length definition.

The OSF persistence length also has an almost constant regime, with a salt-free limit

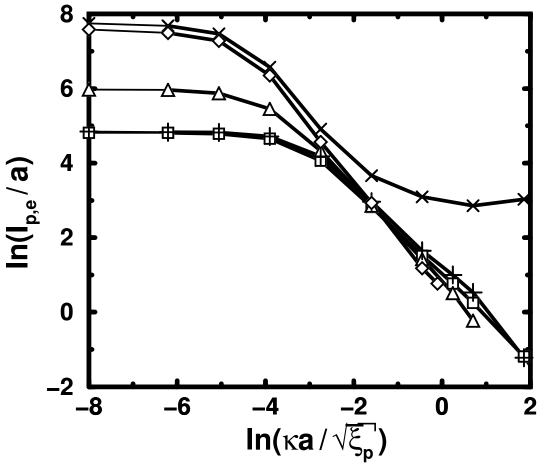

FIG. 5. The logarithm of the electrostatic persistence length as a function of the logarithm of $\kappa a/\sqrt{\xi_p}$ for different definitions of $l_{p,e}$: $l_{p,N/2} - a$ from Eq. (2) (plus signs), $l_{p,R} - a$ from Eq. (5) (squares), $l_{p,x} - a$ from Eq. (6) (crosses), $l_{p,\infty} - a$ from Eq. (7) (diamonds), $l_{p,w} - a$ from Eq. (11) (triangles). The values are based on simulation results, either directly or through R_{ee}, of 320-mers with $a = 3$ Å.

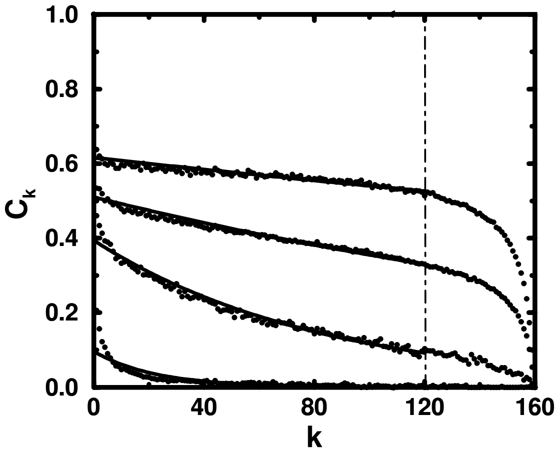

FIG. 6. The orientational correlation function for a 320-mer with $a = 12$ Å and salt concentrations of 0, 0.1, 1, 100 mM (top to bottom) represented by small circles. The solid lines are exponentials fitted in the range k=0–120. The dot-dashed line just shows the upper limit of the fitting and the upper limit of the y-axis is a reminder that $C_0 = 1$.

$l_{OSF} = l_B Z^2/72$ (see Fig. 7). In this region the value of the electrostatic persistence length is sensitive to whether it includes end-effects, like $l_{p,i}$ and $l_{p,R}$, or is defined through a correlation function that is extrapolated to infinite chain lengths, like $l_{p,\infty}$ (and in principle $l_{p,x}$ if C_0 is close to one, cf. Eq. (7)). l_{OSF} belongs to the latter group and is actually in fair agreement with $l_{p,\infty}$ (and $l_{p,x}$) in this regime (see Table I). The worm-like chain expression, Eq. (11), gives a behaviour intermediate between the two extremes and since

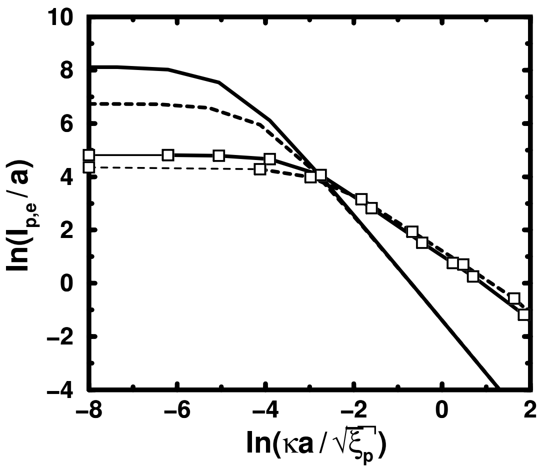

FIG. 7. OSF theory [Eq. (16)] (no symbols) compared to the simulated electrostatic persistence length, $l_{p,e} = l_{p,R} - a$ from Eq. (5), (squares). The results are for 320-mers with $a = 3$ Å (solid lines) and $a = 12$ Å (dashed lines). The values on the y-axis are the results for the salt-free case.

the worm-like chain is often used to obtain persistence lengths from experimental data this is the behaviour expected to be reported experimentally. Such a report by Förster *et al.* appears to be at odds with both OSF theory and the notion of a power law for the κ dependence,[40] but a comparison with the results here suggests that their experimental system just displays the constant regime and the subsequent cross-over region. This means that their comparison with OSF theory is rather unfair since they are using the high-salt version, Eq. (18).

In the second regime, l_{OSF} of course displays the well-known quadratic dependence on the Debye length, in disagreement with simulations. It is interesting to note that l'_{OSF}/a has the correct relationship between ξ_p and κa. It is essentially the square of the dimensionless form of the right-hand side of Eq. (30). This is a little bit tricky, however. Going from Eq. (17) to Eq. (18) the choice of the bond length a is arbitrary, because it is always balanced by α. This is no longer true if we are to scale l'_{OSF} by a. In that case we need the proper rigid bond model to get the correct bond length dependence, which is closely related to the above discussion about the difference between having an effective charge or an effective bond length, *i.e.* using ξ_p or the Manning parameter, ξ.

Figure 8 shows that the electrostatic persistence length obtained from the variational calculations is slightly higher than the simulation results for the same model. Otherwise, the agreement is excellent. The calculations have been made for a flexible bond chain with $r_0 = 6$ Å and the root-mean-square bond length is around 12 Å, a little longer at low salt concentrations and a little shorter at high screening. As the simulation results show the behaviour is almost identical to that of a rigid bond chain with $a = 12$ Å. It is a general conclusion that models with flexible, harmonic bonds give the same results as rigid bond chains if the the actual, simulated root-mean-square monomer-monomer separation is used

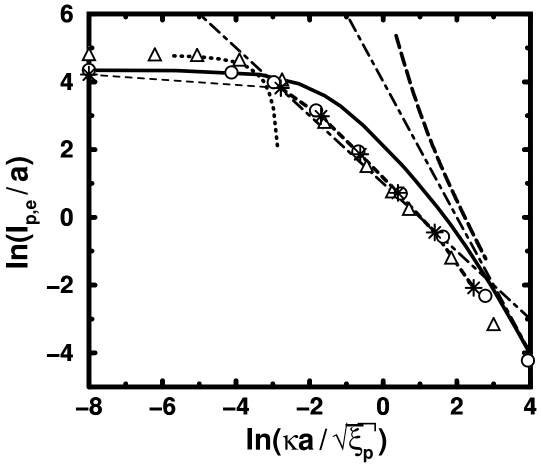

FIG. 8. Comparison between simulations and variational and perturbational calculations. The simulation results are for 320-mers with rigid bonds of 3 Å (triangles) and 12 Å (circles) and flexible bonds with $r_0 = 6$ Å (dashed line, stars). The solid line represent the variational result for the latter, while the dotted line and the long dashed lines are low temperature and high temperature expansions, respectively, for a 512-mer with $r_0 = 6$ Å. The *symbols* on the y-axis are for the salt-free case and the dot-dashed lines mark a slope of -1 and -2, respectively.

to represent the bond length. A pair similar to $r_0 = 6$ Å$/a = 12$ Å is $r_0 = 9$ Å$/a = 24$ Å.

When the Debye length is on the order of the bond length ($\kappa a \approx 1$) the variational result crosses over to a third regime where $l_{p,e}$ is proportional to κ^{-2}, i.e. we get a behaviour similar to the OSF prediction, which applies to stiff chains. Although the chain is highly flexible, it is stiff on the length scale of a bond and when κ^{-1} is of this order, the intrinsic persistence length, $l_{p,0} = a$, dominates the total persistence length. The OSF theory treats the electrostatic interactions as a perturbation to an intrinsic bending energy, which is quadratic in the bending angle. Analysing the high temperature expansion, Eq. (24), which is also a perturbational calculation, we would get a κ^{-2} dependence to the lowest order for the entire range of salt concentrations if $l_{p,e}$ were plotted as a function of $\sqrt{\xi_p}/\kappa$, but scaling with the bond length as in Fig. 8 the expansion result curves upwards at lower salt concentrations.

The simulation results appear also to cross over into a third regime at (ridiculously) high salt concentrations, although the exponent of κ^{-1} seems to be closer to 1.5 and slowly increasing. Seidel's large exponent, also 1.5, for κ^{-1} may be due to the fact that the Debye length was smaller than the distance between neighbouring charges.[24]

Finally, the low temperature expansion, which corresponds to a rigid rod, gives the expected almost constant persistence length at low salt concentrations, but diverges when $\kappa R_{ee} \approx 1$ and the chain cannot bend as it is supposed to.

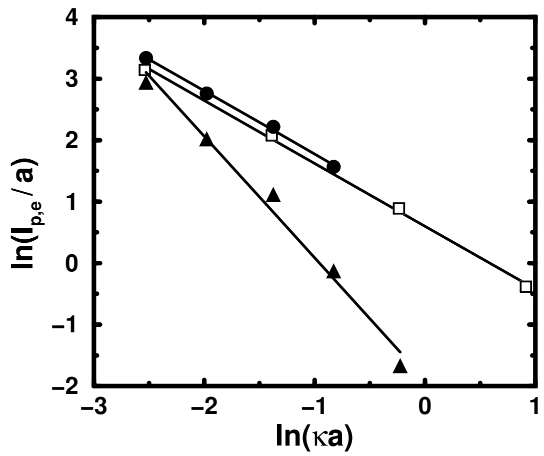

FIG. 9. The electrostatic persistence length for a 320-mer with rigid bonds of a = 24 Å and an angular potential with $l_A = \sqrt{2000}$ Å (filled circles) and $l_A = \sqrt{20000}$ Å (filled triangles). The solid lines are least square fits, which have the slopes -1.0 and -2.0, respectively. Also shown is the corresponding chain without the angular potential (open squares).

B. Stiff polyelectrolyte

Thus, we have shown that the OSF theory is not applicable for a flexible polyelectrolyte where the electrostatic persistence length is of the same order as the total persistence length. This should not come as a surprise, since the OSF theory was derived for a chain with a significant intrinsic stiffness and where the electrostatic persistence length only gives a minor contribution to the total persistence length.

One way to introduce a non-electrostatic stiffness beyond the bond length is via an angular potential [see Eq. (20)]. We have performed such simulations for a fully charged chain with 320 monomers and a fixed bond length a = 24 Å and found that the persistence length still scales like κ^{-1}. With increasing l_A, however, the dependence changes over to κ^{-2} in agreement with the OSF result. Figure 9 shows how a chain with $l_A = \sqrt{2000}$ Å and with an intrinsic persistence length, $l_{p,0} = 83$ Å decays like κ^{-1}, just like the flexible chain without the angular potential, i.e. $l_A = 0$ Å. Upon increasing the stiffness to $l_A = \sqrt{20000}$ Å and a $l_{p,0} = 759$ Å the κ dependence shifts to -2. The κ dependence at high salt concentration still seems to be quadratic although considerable numerical difficulties prevent an accurate analysis.

VI. CONCLUSIONS

Simulating a flexible polyelectrolyte model that only has screened Coulomb interactions, besides the bond interactions, we find a linear relationship between the electrostatic persistence length and the Debye length in the controversial region where the Debye length is shorter than the chain dimensions ($\kappa^{-1} \ll R_{ee}$) and the interactions have become more local. Furthermore, we also find that the electrostatic persistence length is proportional to the square root of the strength parameter $\xi_p = \alpha^2 l_B/a$, which measures the internal interactions, i.e we have $l_{p,e} \sim \sqrt{\xi_p}/\kappa$. This is in agreement with experiment, but contradicts OSF theory, which predicts $l_{p,e} \approx \alpha^2 l_B/(2\kappa a)^2$.

The conclusions remain the same if different definitions of persistence length are used, although $l_{p,x}$ [Eq. (6)] may give erratic results when obtained by a simple fitting to the orientational correlation function.

Variational calculations agree with simulations. A small difference is seen at very high salt concentrations, where the variational results predict a κ^{-2} dependence as in the OSF theory. Here simulations give an exponent p between 1 and 2 for $l_{p,e} \sim \kappa^{-p}$. In this region, $\kappa^{-1} \ll a$, and the electrostatic interactions can be treated as a small perturbation to the harmonic interactions in the variational ansatz, similar to the perturbation of the quadratic bending energy in the OSF theory. A high temperature expansion carried to first order gives a quadratic dependence throughout the concentration range.

Finally, for a stiff chain where the electrostatic persistence length only gives a minor contribution to the the total stiffness, we find that theory due to Odijk and Skolnick and Fixman is valid. Under these conditions the electrostatic persistence length scales like κ^{-2}.

[1] J. P. Valleau, Chem. Phys. **129**, 163 (1989).
[2] H. H. Hooper, H. W. Blanch, and J. M. Prausnitz, Macromolecules **23**, 4820 (1990).
[3] C. E. Reed and W. F. Reed, J. Chem. Phys. **94**, 8479 (1991).
[4] G. A. Christos, S. L. Carnie, and T. P. Creamer, Macromolecules **25**, 1121 (1992).
[5] M. J. Stevens and K. Kremer, J. Chem. Phys. **103**, 1669 (1995).
[6] C. Seidel, H. Schlacken, and I. Müller, Ber. Bunsenges. Phys. Chem. **100**, 175 (1996).
[7] T. Åkesson, C. Woodward, and B. Jönsson, J. Chem. Phys. **91**, 2461 (1989).
[8] T. Wallin and P. Linse, J. Phys. Chem. **100**, 17873 (1996).
[9] T. Odijk, J. Polym. Sci., Polym. Phys. Ed. **15**, 477 (1977).
[10] J. Skolnick and M. Fixman, Macromolecules **10**, 944 (1977).
[11] J.-L. Barrat and J.-F. Joanny, Europhys. Lett. **24**, 333 (1993).
[12] B. Y. Ha and D. Thirumalai, Macromolecules **28**, 577 (1995).
[13] U. Micka and K. Kremer, Phys. Rev. E **54**, 2653 (1996).
[14] U. Micka and K. Kremer, personal communication .
[15] G. Maret and G. Weill, Biopolymers **22**, 2727 (1983).
[16] H. Mattoussi, S. O'Donohue, and F. E. Karasz, Macromolecules **25**, 743 (1992).
[17] T. Odijk and A. C. Houwaart, J. Polym. Sci., Polym. Phys. Ed. **16**, 627 (1978).
[18] A. R. Khokhlov and K. A. Khachaturian, Polymer **23**, 1742 (1982).

[19] M. Tricot, Macromolecules **17**, 1698 (1984).
[20] S. Ghosh, X. Li, C. E. Reed, and W. F. Reed, Biopolymers **30**, 1101 (1990).
[21] W. F. Reed, S. Ghosh, G. Medjahdi, and J. Francois, Macromolecules **24**, 6189 (1991).
[22] V. Degiorgio, F. Mantegazza, and R. Piazza, Europhys. Lett. **15**, 75 (1991).
[23] M. Schmidt, Macromolecules **24**, 5361 (1991).
[24] C. Seidel, Macromol. Theory Simul. **3**, 333 (1994).
[25] O. Kratky and G. Porod, Recl. Trav. Chim. Pays-Bas **68**, 1106 (1949).
[26] H. Yamakawa, *Modern Theory of Polymer Solutions* (Harper and Row, New York, 1971).
[27] M. Schmidt, Macromolecules **17**, 553 (1984).
[28] N. A. Metropolis, A. W. Rosenbluth, M. N. Rosenbluth, A. Teller, and E. Teller, J. Chem. Phys. **21**, 1087 (1953).
[29] M. Lal, Mol. Phys. **17**, 57 (1969).
[30] N. Madras and A. D. Sokal, J. Stat. Phys. **50**, 109 (1988).
[31] M. Bishop, J. H. R. Clarke, A. Rey, and J. J. Freire, J. Chem. Phys. **95**, 4589 (1991).
[32] B. Jönsson, C. Peterson, and B. Söderberg, J. Phys. Chem. **99**, 1251 (1995).
[33] M. Ullner, B. Jönsson, and P.-O. Widmark, J. Chem. Phys. **100**, 3365 (1994).
[34] M. Ullner, B. Jönsson, B. Söderberg, and C. Peterson, J. Chem. Phys. **104**, 3048 (1996).
[35] B. Söderberg, unpublished .
[36] C. Peterson, O. Sommelius, and B. Söderberg, J. Chem. Phys. **105**, 5233 (1996).
[37] G. S. Manning, J. Chem. Phys. **51**, 924 (1969).
[38] M. Ullner and B. Jönsson, Macromolecules **29**, 6645 (1996).
[39] P. J. Flory, *Principles of Polymer Chemistry* (Cornell University Press, Ithaca, 1992).
[40] S. Förster, M. Schmidt, and M. Antonietti, J. Phys. Chem. **96**, 4008 (1992).